Available online at www.sciencedirect.com

ScienceDirect

Energy Procedia 74 (2015) 1220 – 1227

Energy Procedia

International Conference on Technologies and Materials for Renewable Energy, Environment and Sustainability, TMREES15

Numerical simulation of CGS/CIGS single and tandem thin-film solar cells using the Silvaco-Atlas software

M. Elbar* and S. Tobbeche

Laboratoire des Matériaux Semi-conducteurs et Métalliques, Faculté des Sciences et de la Technologie, Département de Génie-Electrique, Université de Biskra, B.P 145, Biskra 07000, Algérie.

Abstract

In this work, numerical simulations of single and double junction solar cells based copper gallium diselenide (CGS) and copper indium gallium diselenide (CIGS) electrical characteristics are performed using a physically based two-dimensional device simulator Silvaco-Atlas. The J-V characteristics and the external quantum efficiency EQE are simulated under AM1.5 illumination. In this study, where the single CGS solar cell used as the top cell and the single CIGS solar cell used as the bottom cell in the tandem configuration show conversion efficiencies of 18.92% and 20.32%, respectively. Our simulation results of the CIGS solar cell are in good agreement with the experimental high record efficiency. The simulated photovoltaic parameters of the CGS/CIGS tandem cell are: the short-circuit current density J_{sc} of 16.35 mA/cm^2, the open circuit voltage V_{oc} of 1.8 V and the fill factor FF of 85.09 % and the conversion efficiency η of 25.11%. In the CGS/CIGS tandem solar cell, an improvement in the conversion efficiency to 25.11% was found. The overall investigation on copper indium gallium diselenide solar cells gives potential suggestions that may lead to the fabrication of the high efficiency CGS/CIGS single and tandem solar cells.

Peer-review under responsibility of the Euro-Mediterranean Institute for Sustainable Development (EUMISD)

Keywords: numerical simulation;Silvaco-Atlas;CGS solar cell;CIGS solar cell;CGS/CIGS tandem cell;efficiency.

1. Introduction

Thin film solar cells have the potential for low-cost and large-scale terrestrial photovoltaic applications. A number of semiconductor materials including polycrystalline CdTe, CIGS and amorphous silicon (a-Si) materials have been

* Corresponding author. Tel.:+21333543199; fax: +21333543199.
*E-mail address:*elbarmourad@gmail.com

Peer-review under responsibility of the Euro-Mediterranean Institute for Sustainable Development (EUMISD)
doi:10.1016/j.egypro.2015.07.766

developed for thin-film photovoltaic solar cells. The polycrystalline Copper-indium-gallium-diselenide (CIGS) thin film is a member of the I–III–VI2 group of chalcopyrite semiconductors, and achieve the highest conversion efficiency compared to other Cu-chalcopyrite thin film solar cells as well as CdTe and amorphous Si thin film solar cells. The CIGS material is a suitable energy band gap semiconductor with a high optical absorption coefficient in the visible spectrum of incident sunlight, the absorption coefficient of CIGS films in the visible spectrum is 100 times larger than silicon material. Furthermore, the CIGS thin film solar cell exhibits a tunable band-gap, an excellent outdoor stability, radiation hardness and it offers a specific power up to 919 W/Kg, the highest for any solar cell. Recently, CIGS thin film solar cell with an active area of 0.5 cm^2 exhibits the highest efficiency of 20.3% in the Centre of Solar Energy and Hydrogen Research (ZSW) [1] and 19.9% in National Renewable Energy Laboratory (NREL) [2]. The band-gap energy of the $Cu(In_{(1-x)},Ga_x)Se_2$ (CIGS) films varies in the range from 1.04 to 1.68 eV with the corresponding Ga content in the CIGS films from x = 0 to 1[3]. An increase in efficiency is expected mainly using denominated tandem, triple, and multi-junction solar cells, consisting of layers with different band-gap energies in order to utilize different energy regions of the solar spectrum. In this context, several researchers are trying to fabricate reliable cells with wide band gaps in order to use them as top cells. Tandem solar cell consists of the top high-bandgap cell, which absorbs the short-wavelength (high-energy) part of the spectrum, and the bottom low-bandgap cell absorbing the rest. Synthesis and physical properties of CIGS nanoparticles and $CuGaSe_2$ (CGS) thin films for tandem cell PV applications show that the optical band-gap of the nanoparticles is increased when they grow at high temperature. Furthermore, modeling and simulation of a CGS/CIGS tandem solar cell have shown efficiency of 25% [4] and for a CdZnTe/CIGS cell, 26% [5]. Modeling of a low-cost organic–inorganic hybrid tandem PV cell to achieve efficiencies exceeding 20% have also been proposed [6]. The development of mechanically stacked and monolithically integrated tandem cells, using a bottom CIGS cell and a top dye-sensitizer solar cell (DSC), as well different methods to increase the transmittivity of the top cell, have also been studied [7]. The tandem cell of DSC and CIGS was first made by Gratzel with conversion efficiency greater than 15% [8], and 12.35% [9] and 10.46% [10]. Moreover, the fabrication of mechanical stacked tandem device with an $Ag(In,Ga)Se_2$ (AIGS) top cell and a CIGS bottom cell show an open circuit voltage of 1.5 V [11], and As to CIGS, the band-gap of $CuGaSe_2$ (1.68 eV) ideally satisfies the requirements for the top cell. Series-connected $CuGaSe_2$/$CuInGaSe_2$ tandem cell was reported to achieve a high open-circuit voltage of 1.18V with the conversion efficiency of 7.4% [12].

In this work, we have used the Silvaco-Atlas software [13] on the design and the study of single and double junction solar cells based copper indium gallium diselenide (CIGS). Firstly, we will report the modeling and simulation results of CGS/CIGS single junction solar cells, in comparison with the previously reported experimental results. Secondly, we will show the simulation results of a CGS/CIGS tandem solar cell which exhibits an improvement in the photovoltaic performance compared to the CGS/CIGS single solar cells. This work will also contribute to obtain a better understanding and insight in CGS/CIGS single and tandem solar cells.

2. CGS/CIGS tandem solar cell structure and numerical simulation

Higher efficiencies could be obtained by stacking together different absorbers with different bandgaps to maximize the light absorption. The basic structure of the CGS/CIGS tandem solar cell is shown in Fig. 1.

It consisted of two solar cells where the CGS wide bandgap top cell had a small thickness and a large band gap (E_g=1.69 eV) in contrast to the CIGS low band-gap bottom cell, which had a usual thickness for a CIGS cell and a band- gap value (E_g=1.16 eV) close to the optimal values of best cells [1]. This design is intended to convert a wider range of photons incident on the solar cell and generate therefore a maximum power output. The tandem cell consisted of a top n-CdS/p-CGS heterojunction and a bottom n-CdS/p-CIGS heterojunction. The top CGS and the bottom CIGS cells are optically and electrically connected with a transparent conducting oxide layer (TCO) of ZnO. The tandem solar cell was considered illuminated under AM 1.5 solar spectrum with 100 $mW.cm^{-2}$ incident power density which was assumed to be normally incident on the top ZnO layer used as the cathode contact to the bottom metallic Molybdenum (Mo) forming the back anode contact of the tandem solar cell. The acceptor concentration in CIGS is generally around $2x10^{16}$ cm^{-3} [14], and we chosed $2x10^{16}$/$8x10^{16}$ cm^{-3} for CGS/CIGS in this study. The doping concentrations of donors and acceptors and thicknesses of the layers used in the simulation are indicated in Fig. 1.

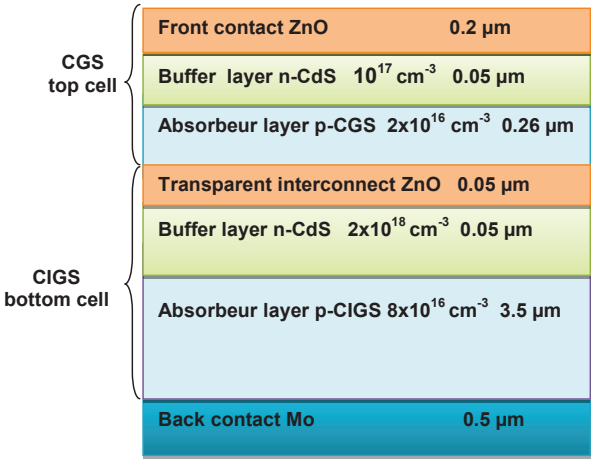

Fig. 1 Tandem solar cell with CGS/CIGS subcells connected by transparent interconnect ZnO, the relative doping concentrations and the thicknesses are listed for each layer.

The software Silvaco Atlas-2D requires the input of the device parameters which are those of material parameters of each layer in the cell structure. The semiconductor properties of CdS, CGS (CIGS) layers used as the input parameters for the simulations were given in Table1.
An approximate expression of the band gaps of the semiconductors $Cu(In_{(1-x)},Ga_x)Se_2$ alloys was used [15].

$$E_g(x) = 1.011 + 0.664x - 0.249(1-x) \tag{1}$$

Where E_g ranging from 1.011 eV to 1.68 eV for x=0 (CIS) and x=1 (CGS), respectively.

The electron mobility μ_n and hole mobility μ_p of each layer were set according to [16] and [14]. The electron affinity χ_e of $CuInGaSe_2$ was reported to be in the range of 4.10–4.90 eV [3] and 4.8 eV was chosen for the simulation. The effective density of states of the conduction band N_c and of the valence band N_v, respectively, of each layer were set according to [17].

All the layers are polycrystalline and therefore contain a large number of different defects [18]. According to [14], we considered two Gaussian deep donor defect distributions for the (CGS/CIGS) layers and a Gaussian deep acceptor defect distribution for the CdS layer [13, 19].

$$g_{GA}(E) = N_{GA} \exp\left(-\left(\frac{E_{GA}-E}{W_{GA}}\right)^2\right) \tag{2}$$

$$g_{GD}(E) = N_{GD} \exp\left(-\left(\frac{E-E_{GD}}{W_{GD}}\right)^2\right) \tag{3}$$

Where E is the defect energy, the subscripts (G, A, D) stand for Gaussian acceptor and donor defect states, respectively. The density of states is described by its effective density of states (N_{GA} and N_{GD}), its standard energy deviation (W_{GA} and W_{GD}), and its peak energy position (E_{GA} and E_{GD}).

The position of the recombinative defect states is in a narrow distribution close to the middle of the band gap [18, 20]. Shockley-Read-Hall (SRH) recombination model for the defects implemented in Silvaco for device simulation is used to calculate carrier recombination rates which depend on the density of states present within the band-gap, the defect energy level and electron and hole capture cross sections. The electron/hole capture cross section (σ_n/σ_p) can range between 10^{-18} and 10^{-15} cm^2 [14], and were chosen for the simulation of CGS/CIGS ($2x10^{-15}/3x10^{-13}$) and CdS ($10^{-15}/10^{-17}$). Defect recombination at the semiconductor heterointerfaces (e.g. CdS/CGS, CdS/CIGS) and at the front and back contacts are modeled by the inclusion of surface recombination velocities of both electrons (S_e) and

holes (S_h) and chosen equal to 10^5 cm/s. The optical parameters of the real and the imaginary parts of the refractive index $n(\lambda)$ and extinction coefficient $k(\lambda)$ of the CGS/CIGS materials are obtained from [21] and for ZnO and CdS layers, they can be found in [22, 23]. For metal contact layer (Mo), optical constants available in the SOPRA database of the Silvaco-Atlas software were used in the simulation. Reflection loss from the surface of the tandem solar cell has also been integrated into the model. In this study, the solar cells operating temperature was set at 300 K.

Table1 Material parameters used in the simulation. In the table (A) and (D) denote acceptor and donor defects.

Layer Properties	CdS	CGS/CIGS
Layer band gap E_g (eV)	2.4	1.69/1.16
Electron affinity χ_e (eV)	4.5	4.8
Relative permittivity ε_r (F.cm^{-1})	10	13.6
Electron mobility μ_n (cm^2/V.s)	100	100
Hole mobility μ_p(cm^2/V.s)	25	25
Conduction band effective density of states N_c (cm^{-3})	2.2x10^{18}	2.2x10^{18}
Valence band effective density of states N_v (cm^{-3})	1.8x10^{19}	1.8x10^{19}
Gaussian defect states		
Gaussian defect density N_{GA}, N_{GD} (cm^{-3})	10^{15}(A)	10^{15}(D)
Peak energy position E_{GA}, E_{GD} (eV)	1.2 (A)	0.84/0.58(D)
Standard energy deviation W_{GA}, W_{GD} (eV)	0.1(A)	0.1(D)
Electron capture cross section σ_n (cm^2)	10^{-15}	2x10^{-15}
Hole capture cross section σ_p (cm^2)	10^{-17}	3x10^{-13}
Surface recombination velocity for electrons (holes) (cm.s^{-1})		
at CdS/CIGS interface	10^5	10^5
at CdS/CGS interface	10^5	10^5
at front contact	10^5	10^5
at back contact	10^5	10^5

3. Results and discussions

The CIGS and CGS single solar cells are first simulated individually. The simulation parameters are shown in Table 1.

3.1. Modeling of a CIGS single bottom cell

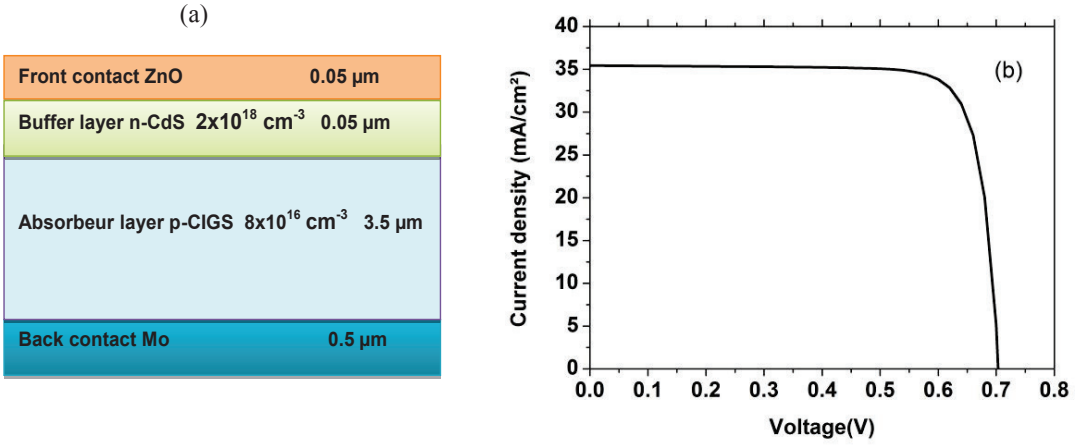

Fig. 2 (a) CIGS single bottom cell structure, (b) J-V characteristic for the CIGS single bottom cell.

The simulated CIGS single bottom solar cell structure is shown in Fig. 2 (a). It is formed by a p-type CIGS absorber and an n-type CdS (buffer), a transparent contact of ZnO layer is deposited on the top of the structure, the solar cell structure is completed by molybdenium Mo rear metallization contact. The Ga composition is about 0.31, corresponding to band-gap energy of 1.16 eV. The simulated CIGS solar cell structure is similar to that achieved experimentally in [1]. The cell setup was described as follows: soda-lime glass (3 mm), sputtered molybdenum (500–900 nm), CIGS (2.5–3.5 μm), chemical bath deposited CdS buffer layer (40–50 nm), sputtered undoped ZnO (50– 100 nm), sputtered aluminium doped ZnO (150–200 nm) and nickel/aluminium-grid. CIGS solar cells with an efficiency of 20.3% were produced with varying composition (Ga / (Ga +In)) from 0.30 to 0.35 [1].

After the adjustment of the doping concentrations of the CdS and CIGS layers as indicated in fig.2 (a), J-V characteristic is presented in Fig. 2 (b) and our simulation results are compared to the simulation and experimental results [24, 1] in Table 2. From these results, we can see that our simulated results are in good agreement with simulation and experimental results in [24, 1], thus validating our model and the parameters used in the simulation.

Table 2 Simulation and experiment parameters of a CIGS single bottom solar cell.

	J_{sc}(mA/cm^2)	V_{oc} (V)	FF (%)	η (%)
CIGS single bottom cell simulation	35.44	0.709	80.69	20.32
CIGS solar cell simulation [24]	41.1	0.64	77.33	20.34
Experiment [1]	35.4	0.74	77.5	20.3

3.2. Modeling of a CGS single top cell

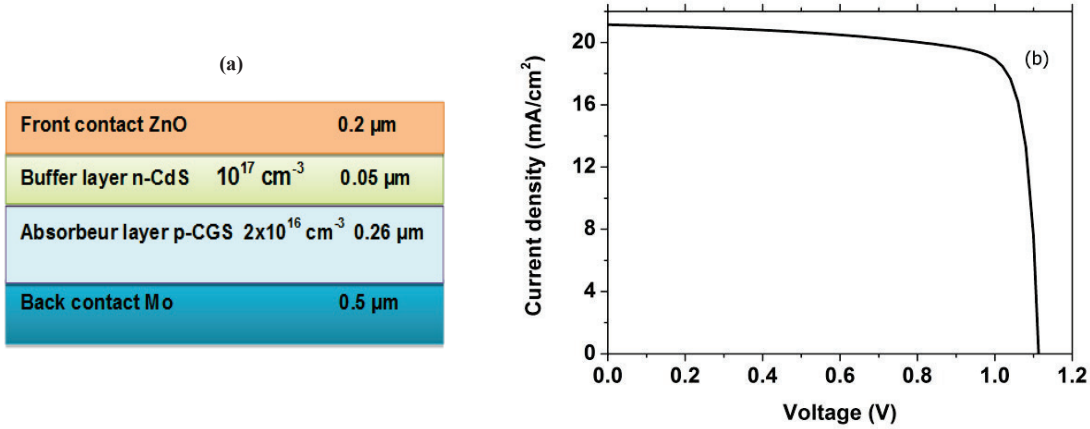

Fig. 3 (a) CGS single top solar cell structure, (b) J-V characteristic for the CGS single top solar cell.

Our simulated solar cell structure is formed by a p-type CGS absorber and an n-type CdS buffer, a transparent contact of ZnO layer is deposited on the top of the structure and the solar cell structure is completed by molybdenium Mo as a back contact. In Fig. 3 (a) is shown the CGS single junction solar cell structure. The Ga composition is about 1, corresponding to band-gap energy of 1.69 eV. The structure was optimized to improve the conversion efficiency. J-V characteristic is presented in Fig. 3 (b) and the simulated photovoltaic parameters are summarized in Table 3.

Table 3 Simulated photovoltaic parameters of a CGS single top solar cell.

	J_{sc}(mA/cm^2)	V_{oc} (V)	FF (%)	η (%)
CGS single top cell	21.13	1.11	80.42	18.92

3.3. Modeling of a CGS/CIGS tandem cell

The CGS/CIGS tandem solar cell structure simulated is shown in Fig. 1. Fig. 4 shows the J–V characteristics of the top, bottom, and tandem solar cells and their photovoltaic parameters are indicated in Table 4. In order to extract the J-V curves and the photovoltaic parameters of the top and the bottom cell of the tandem cell, two sets of anodes and cathodes were used. The anode and the cathode of the top cell were placed at the bottom of the CGS layer and the front contact ZnO, respectively. For the bottom cell, the anode and the cathode were set at the back contact Mo and the transparent interconnect ZnO, respectively.

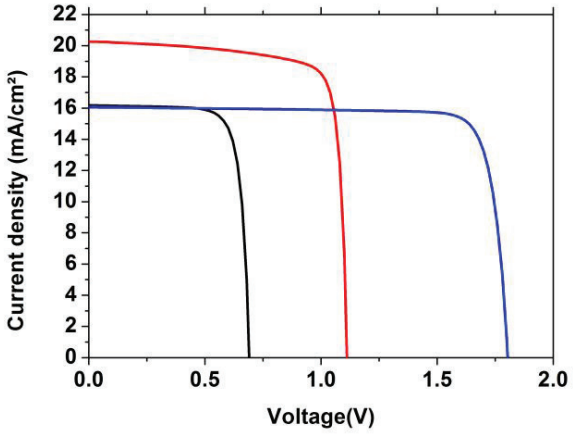

Fig. 4 J-V characteristics for the CGS top cell, CIGS bottom cell and CGS/CIGS tandem cell.

The CGS/CIGS tandem solar cell works successfully. The J_{sc} of the tandem cell is limited by the low current of the CIGS bottom cell, the tandem short circuit current density of 16.35 mA/cm^2 approaches the short circuit current density of the bottom cell (J_{sc}=16.17 mA/cm^2) and the open circuit voltage of 1.8 V is the summation of the open circuit voltages of the CGS and CIGS cells (1.11V and 0.69 V). From these results, we can see the correct operation of the series connected CGS and CIGS cells forming the tandem cell. In addition, the fill factor of the tandem cell (85.09%) is higher than the CGS and CIGS cells fill factors (80.94% and 79.05%). Increased open circuit voltage and fill factor enhance the conversation efficiency of the tandem cell to 25.11% which is higher than those of the single CIGS and CGS cells (20.3% and 18.92%). Compared to previous simulation studies by employing AMPS-1D software, tandem cells based on CIGS and CGS cells achieve optimum conversion efficiencies of 25% [4] and 24% [15] using Silvaco-Atlas software, our simulated GGS/CIGS tandem cell conversion efficiency of 25.11% is close to those in [4, 15].

Table 4 Photovoltaic parameters of the top, bottom and tandem solar cells.

	J_{sc}(mA/cm^2)	V_{oc} (V)	FF (%)	η (%)
CGS top cell	20.26	1.11	80.94	18.22
CIGS bottom cell	16.17	0.69	79.05	8.83
CGS/CIGS tandem cell	16.35	1.8	85.09	25.11

By comparing the photovoltaic parameters of the CIGS single bottom cell and the CIGS bottom cell, we observe that the photovoltaic parameters of the CIGS bottom cell have degraded due to the top layers absorbing some of the incident light. The same for the photovoltaic parameters of the CGS single top cell and the CGS top cell, a small decrease of the photovoltaic parameters of the CGS top cell due to the small bottom layers absorption of the incident light.

The curves of the external quantum efficiency (EQE) versus wavelength for both the top and bottom cells of the tandem solar cell are shown in Fig. 5. We have simulated EQE under short-circuit mode. The top cell shows a maximum in the EQE around 0.38 µm, while the bottom cell shows a maximum in EQE at 0.83 µm. The short wavelength region below 0.7 µm is mostly absorbed in the top cell while the wavelength range between 0.78 and 1.1µm is absorbed in the bottom cell.

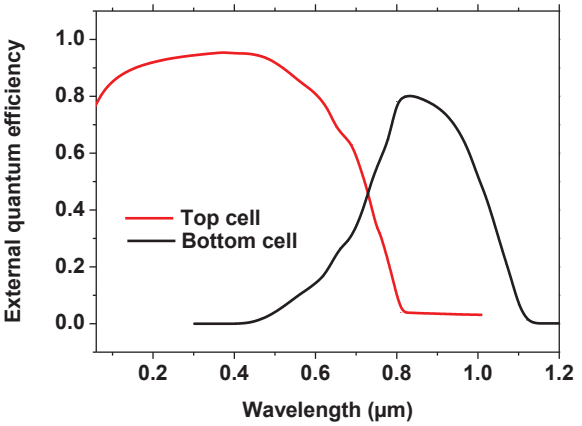

Fig. 5 EQE of the CGS/CIGS tandem solar cell as function of wavelength

4. Conclusion

Based on the Silvaco-Atlas software, we presented numerical simulations of single junction CIGS and CGS solar cells as well as two terminal CGS/CIGS tandem solar cell, under AM1.5. J-V characteristics and external quantum efficiency were presented. We first simulated and determined the optimized CIGS bottom solar cell with conversion efficiency around 20.3% in agreement with the high record conversion efficiency found experimentally in the CIGS solar cell. In the second step, we simulated the CGS top cell and the tandem cell. In the case of the tandem CGS/CIGS solar cell, an improvement in the conversion efficiency to 25.11% was found. In this study, we have investigated by simulation the photovoltaic performance that might be achieved by single junction CGS and CIGS solar cells and CGS/CIGS tandem solar cell, numerical simulations performed in this work would contribute to designing and fabricating high efficiency CGS/CIGS single and tandem solar cells.

References

[1] Jackson P, Hariskos D, Lotter E, Paetel S, Wuerz R, Menner R, Wischmann W, Powalla M. New world record efficiency for Cu(In,Ga)Se_2 thin-film solar cells beyond 20%. Prog. Photovolt. Res. Appl. 2011; 19: 894- 897.

[2] Repins I, Contreras M, Romero M, Yan Y, Metzger W, Li J, Johnston S, Egaas B, DeHart C, Scharf J. Characterization of 19.9%-efficient CIGS absorbers. 33rd IEEE Photovoltaic Specialists Conference San Diego. California; 2008, May 11–16.

[3] Huang C H. Effects of Ga content on Cu(In,Ga)Se_2 solar cells studied by numerical modeling. Journal of Physics and Chemistry of Solids 2008; 69: 330–334.

[4] Jiyon S, Sheng S Li, Huang C H, Anderson T J, Crisalle O D. Modeling and simulation of a $CuGaSe_2$/Cu(In,Ga)Se_2 tandem solar cell. 3rd World Conference on Photovoltaic Energy Conversion, Osaka, Japan 2003; 1:555-558.

[5] Xiao Y G, Li Z Q, Lestrade M, Simon Li Z M. Modeling of CdZnTe and CIGS and tandem solar cells. 35th IEEE Photovoltaic Specialists Conference, Honolulu, HI, June 20–25, 2010.

[6] Beiley Z, Bowring A, McGehee M D. Modeling low-cost hybrid tandem photovoltaics with power conversion efficiencies exceeding 20%. 38th IEEE Photovoltaic Specialists Conference, Austin, TX, 2012.

[7] Seyrling S, Bucheler S, Chirila A, Perrenoud J, Wenger S , Nakada T, Gratzel M, Tiwari A N. Development of multijunction thin film solar cells. 34th IEEE Photovoltaic Specialists Conference, Philadelphia, PA, 2009.

[8] Liska P, Thampi K R, Gratzel M, Bremaud D, Rudmann D, Upadhyaya H M, Tiwari A N. Nanocrystalline dye-sensitized solar cell/copper indium gallium selenide thin-film tandem showing greater than 15% conversion efficiency. Applied Physics Letters 2006; 88: 203103.

[9] Jeong Woo-Seok, Jin-Wook Lee, SoonilJung , JaeHo Yun, Nam-GyuPark. Evaluation of external quantum efficiency of a 12.35% tandem solar cell comprising dye-sensitized and CIGS solar cells. Solar Energy Materials & Solar Cells 2011; 95: 3419–3423.

[10] Wang WL, Lin H, Zhang J, Li X, Yamada A, Konagai M, Li J B. Experimental and simulation analysis of the dyesensitized solar cell/Cu(In,Ga)Se_2 solar cell tandem structure. Solar Energy Materials & Solar Cells 2010; 94:1753–1758.
[11] TokioNakada, Shunsuke Kijima, YasuhitoKuromiya, Ryota Arai, Yasuyuki Ishii, Nobuyuki Kawamura, Hiroki Ishizaki, Naoomi Yamada. Chalcopyrite thin-film tandem solar cells with 1.5V open circuit-voltage. 2006 IEEE 4th World Conf. on Photovoltaic Energy Conversion, Waikoloa, HI, 2006.
[12] Nishiwaki S, Siebentritt S, Walk P, Lux-Steiner M C. A stacked chalcopyrite thin-film tandem solar cell with 1.2 V open-circuit voltage. Prog. Photovolt.: Res. Appl. (2003); 11: 243–248.
[13] ATLAS User's Manual, Device Simulation Software, SILVACO International, Santa Clara, 2012.
[14] Gloeckler M, Fahrenbruch A L, Sites J R. Numerical modeling of CIGS and CdTe solar cells: Setting the Baseline, in: Proceedings of Third World Conference on Photovoltaic energy Conversion 2003; 1: 491–494.
[15] Konstantinos Fotis. Modeling and simulation of a dual-junction cigs solar cell using silvaco atlas. Master's Thesis, Naval Postgraduate School, Monterey, CA 93943–5000, 2012.
[16] Amin N, Tang M, Sopian K. Numerical modeling of the copper-indium-selenium (CIS) based solar cell performance by AMPS-1D. Proc IEEE 5th Student Conference on Research and Development, Malaysia; 2007, p. 1-6.
[17] Shang X, Wang Z, Mingkai Li, Lei Zhang, Jingang Fang, Jiali Tai, Yunbin He. A numerical simulation study of $CuInS_2$ solar cells. Thin Solid Films 2014; 550: 649–653.
[18] Ouédraogo S, Zougmoré F, Ndjaka J M B. Computational analysis of the effect of the surface defect layer (SDL) properties on Cu(In,Ga)Se_2-based solar cell performances. Journal of Physics and Chemistry of Solids 2014; 75: 688–695.
[19] NebojsaJankovic. Numerical simulations of N-type CdSe poly-TFT electrical characteristics with trap density models of Atlas/Silvaco. Microelectronics Reliability 2012; 52: 2537–25414.
[20] Xunzhong Shang, Zhiqiang Wang, Mingkai Li, Lei Zhang, Jingang Fang, Jiali Tai, Yunbin He. A numerical simulation study of $CuInS_2$ solar cells. Thin Solid Films 2014; 550: 649–653.
[21] Paulson P D, Birkmire R W, Shafarman W N. Optical characterization of $CuIn_{1-x}Ga_xSe_2$ alloy thin films by spectroscopic ellipsometry. J. Appl. Phys. (2003); 94:879-888.
[22] Richter M, Schubbert C, Eraerds P, Riedel I, Keller J, Parisi J, Dalibor T, Avellán-Hampe A. Optical characterization and modeling of $Cu(In,Ga)(Se,S)_2$ solar cells with spectroscopic ellipsometry and coherent numerical simulation. Thin Solid Films 2013; 535: 331–335.
[23] Edward D Palik. Handbook of optical constants of solids III. San Diego, London: Boston Academic press; 1998.
[24] Hossein Movla. Optimization of the CIGS based thin film solar cells: Numerical simulation and analys. Optik 2014; 125:67-70.